

# Decay pathways of stored metal-cluster anions after collisional activation

H. Weidele<sup>1</sup>, M. Vogel<sup>2</sup>, A. Herlert<sup>2</sup>, S. Krückeberg<sup>2</sup>, P. Lievens<sup>1</sup>, R.E. Silverans<sup>1</sup>, C. Walther<sup>3</sup>, and L. Schweikhard<sup>2</sup>

<sup>1</sup>Laboratorium voor Vaste-Stoffysica en Magnetisme, K.U. Leuven, B-3001 Leuven, Belgium

<sup>2</sup>Institut für Physik, Johannes Gutenberg-Universität Mainz, D-55099 Mainz, Germany

<sup>3</sup>Institut für Kernchemie, Johannes Gutenberg-Universität Mainz, D-55099 Mainz, Germany

Received: 1 September 1998 / Received in final form: 22 November 1998

**Abstract.** Size-selected gold clusters,  $\text{Au}_n^-$  ( $n \leq 21$ ), and tungsten clusters,  $\text{W}_n^+$  and  $\text{W}_n^-$  ( $n = 4 - 8$  and  $12$ ), stored in a Penning trap have been collisionally activated. Neutral monomer and dimer evaporation are observed in the case of gold. While no fragment products have been observed for tungsten clusters, there is evidence of electron emission from the anions.

**PACS.** 36.40.c Atomic and molecular clusters – 36.40.Qv Stability and fragmentation of clusters – 34.90.+q Other topics in atomic and molecular collision processes and interactions

## 1 Introduction

Experimental techniques commonly used for the activation of clusters are irradiation with laser light [1–9], collisions with electrons [10, 11], and collisions with nonreactive neutral atoms [12–15]. Activated clusters show fragmentation, electron emission, and radiation. The properties investigated include dissociation pathways and energies, ionization potentials and electron affinities, as well as temperature dependence in the case of the emission of radiation. These characteristics depend on the type and number of constituent atoms and the charge state of the clusters. While radiation always occurs to some extent, it is experimentally found that the particle (electron, monomer, or dimer) with the least separation energy is most favored for emission [6]. From the theoretical point of view, the rate constants for a given dissociation energy and fragmentation process can be calculated from the Rice-Ramsperger-Kassel-Marcus (RRKM) theory [16], and the properties of thermionic electron emission from quasiequilibrium theory [17]. In addition, a modified Stefan-Boltzmann law can be used to describe radiation [8]. Approximations based on these models apply well for many systems [7, 8]. However, the model of thermionic emission of anions seems to need further refinement [17].

In contrast to cations, the actual decay pathways of cluster anions are less obvious, since the activation energies for dissociation and electron emission are in many cases close to each other [6]. Up to now, fragmentation and neutralization studies have been performed for anionic Cu, Al, and Si clusters colliding with Ar and  $\text{SF}_6$ , respectively [15]. Thermionic electron emission has been observed for  $\text{C}_n^-$ ,

$\text{Si}_n^-$  ( $n < 15$ ) and fullerene anions heated by impact on surfaces [18, 19].

The present experiment investigates dissociation and electron emission after collisional activation of gold and tungsten clusters,  $\text{Au}_n^-$ ,  $\text{W}_n^+$  and  $\text{W}_n^-$ , stored in a Penning trap. While most collision experiments using cluster beams allow the determination of the dissociation pathways and bond energies of clusters only within a very limited mass range ( $\sim 1100$  amu) [12], Penning traps have the advantage that clusters of masses up to several thousand amu can be stored and size-selected. In addition, the possibilities for cluster manipulation are manifold, and various cluster studies can be performed without any changes to the apparatus simply by the choice of different experimental event sequences [20]. Dissociation pathways can easily be determined for both anions and cations.

## 2 Experimental procedure

The experimental setup has been described elsewhere [20, 21]. Therefore, its description is restricted to the experimental procedure specific to the observation of the decay pathways of clusters after collisional activation. The setup consists of the following main components: source, trap, and time-of-flight (TOF) section. Cluster ions are produced by a laser vaporization source, which includes a helium carrier gas expansion into the vacuum. After passing several differential pumping stages, the cluster ions are guided to the Penning trap [22] (with magnetic field 5 T, inner diameter 4 cm, trapping voltage 10 V), where they are captured in flight and stored on the time scale

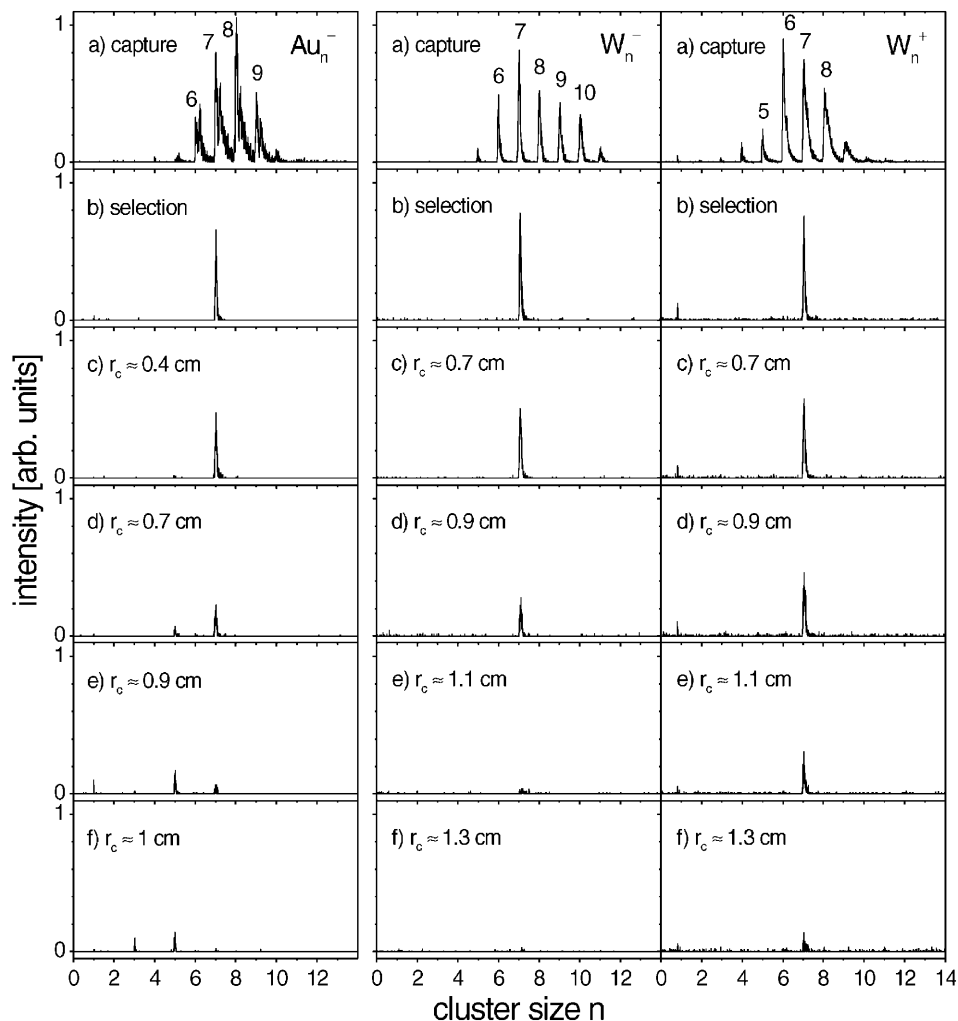


**Fig. 1.** TOF spectra demonstrating the experimental sequence for the cases of  $\text{Au}_7^-$ ,  $\text{W}_7^-$ , and  $\text{W}_7^+$ : (a) cluster size distributions as captured in the trap; (b) after cluster size selection; (c)–(f) after excitation of the cyclotron motion (increasing cyclotron radius  $r_c$  from (c) to (f)).

of seconds for further investigations. After axial ejection through a hole in the endcap electrode of the trap (with a diameter of 5 mm), the reaction products and remaining precursor cluster ions are guided through the TOF drift section to the detector where single ion counting is performed.

The experimental sequence of the collisional activation experiment for both anions and cations is demonstrated by the TOF spectra of Fig. 1. After the capture of the cluster ions (Fig. 1a for  $\text{Au}_n^-$ ,  $\text{W}_n^-$ , and  $\text{W}_n^+$ ; the size range can be chosen by application of appropriate electrostatic potentials for the cluster source and the Penning trap [21]), the selection of one single cluster size is performed by cyclotron resonance ejection of all unwanted ion species (Fig. 1b for  $\text{Au}_7^-$ ,  $\text{W}_7^-$ , and  $\text{W}_7^+$ ). In the next step, the cyclotron motion of the remaining size-selected cluster ions is excited to a given cyclotron radius (and thus kinetic energy) by use of radio-frequency (rf) signals, and subsequently, an argon gas pulse is applied. Due to collisions of the cluster ions with argon atoms, the clusters are given internal energy, and it is expected that, if this energy is high enough, the clusters either dissociate or emit an electron. Increasing the cyclotron radius should result in higher inner energies after the collisions. Indeed, with increasing excitation, the in-

tensity of the precursor signal is reduced, and in the case of gold, the number and intensity of dissociation product species increases (Fig. 1c–f).

The experimental sequence is alternately applied with and without rf irradiation, i.e., with and without collisional activation. The ion intensities from both sequences are compared for the normalization of the dissociation yield. This procedure largely reduces the influence of fluctuations in the cluster production.

## 3 Results

### 3.1 Dissociation pathways of gold cluster anions

As shown in Fig. 1,  $\text{Au}_7^-$  decays into  $\text{Au}_5^-$ , which, for increased excitation, continues to decay into  $\text{Au}_3^-$ . This indicates that small odd-sized gold cluster anions prefer dimer emission when they are activated; this is demonstrated in more detail in Fig. 2, where the normalized signal intensities of the initial cluster  $\text{Au}_7^-$  and the fragments  $\text{Au}_5^-$  and  $\text{Au}_3^-$  are given as a function of the cyclotron radius, which is a measure of the activation energy [23]. The  $\text{Au}_7^-$

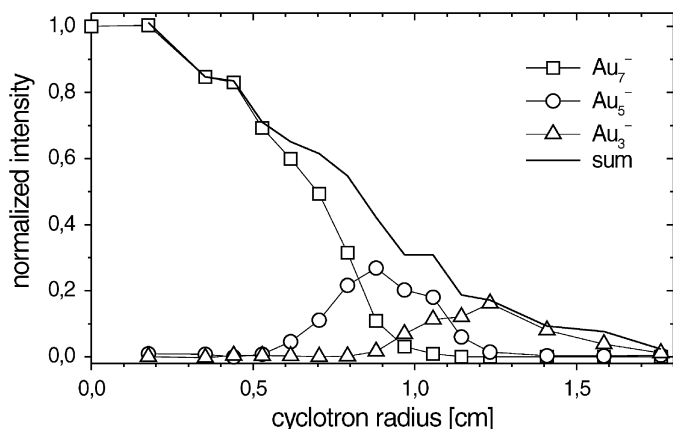


**Fig. 2.** Signal intensity of precursor and fragment clusters as a function of cyclotron radius after collisional activation of  $\text{Au}_7^-$ . The data points are connected to guide the eye.

signal intensity decreases monotonically towards zero with increasing excitation. While  $\text{Au}_7^-$  disappears, the  $\text{Au}_5^-$  intensity rises until it also decreases and is partially replaced by  $\text{Au}_3^-$ . Note that the sum of the intensities of all cluster anions, precursors and fragments is a decreasing function of the cyclotron radius.

The decay pathways of gold clusters,  $\text{Au}_n^-$ , have been investigated for  $n = 2$  to 21. Figure 3 shows TOF spectra for the sizes  $n = 2$  to 15, where the activation has been chosen such as to show the first fragments. Clusters larger than  $n = 11$  evaporate atoms up to  $n = 21$ , the largest clusters investigated. The same behavior is observed for the smaller even-sized clusters. On the other hand, small odd-sized clusters prefer neutral dimer evaporation:  $\text{Au}_{13}^-$ ,  $\text{Au}_{11}^-$ , and  $\text{Au}_9^-$  indicate a transition from monomer to dimer evaporation, the latter being the dominating decay path for  $n \leq 7$ . In the case of  $\text{Au}_{11}^-$  and  $\text{Au}_9^-$ , the signal of  $\text{Au}_{n-1}^-$  is always smaller than the signal of  $\text{Au}_{n-2}^-$ .

### 3.2 Collisional activation of tungsten clusters

Collision experiments have been performed with tungsten clusters,  $\text{W}_n^+$  and  $\text{W}_n^-$ , of size  $n = 4 - 8$  and 12. In contrast to gold anions (and cations [13]), the signals of the  $\text{W}_7^+$  and  $\text{W}_7^-$  clusters are lost upon excitation, and no fragment clusters are observed (Fig. 1). This is a general feature observed for all tungsten clusters under investigation. Figure 4 shows the normalized signal intensities of  $\text{W}_n^\pm$  ( $n = 4 - 8$  and 12) as a function of the cyclotron radius. The signal remains nearly constant up to a certain radius, after which the intensity decreases with increasing radius and approaches zero (with the exception of  $\text{W}_4$ : due to isotopomers that have not been excited [23], there is a remanent intensity). Note that the signal intensity of the anions drops off in a significantly steeper way than that of the cationic clusters. This behavior is most prominent for small clusters, and disappears as the cluster size increases, resulting in almost identical intensity curves for  $\text{W}_{12}^\pm$ .

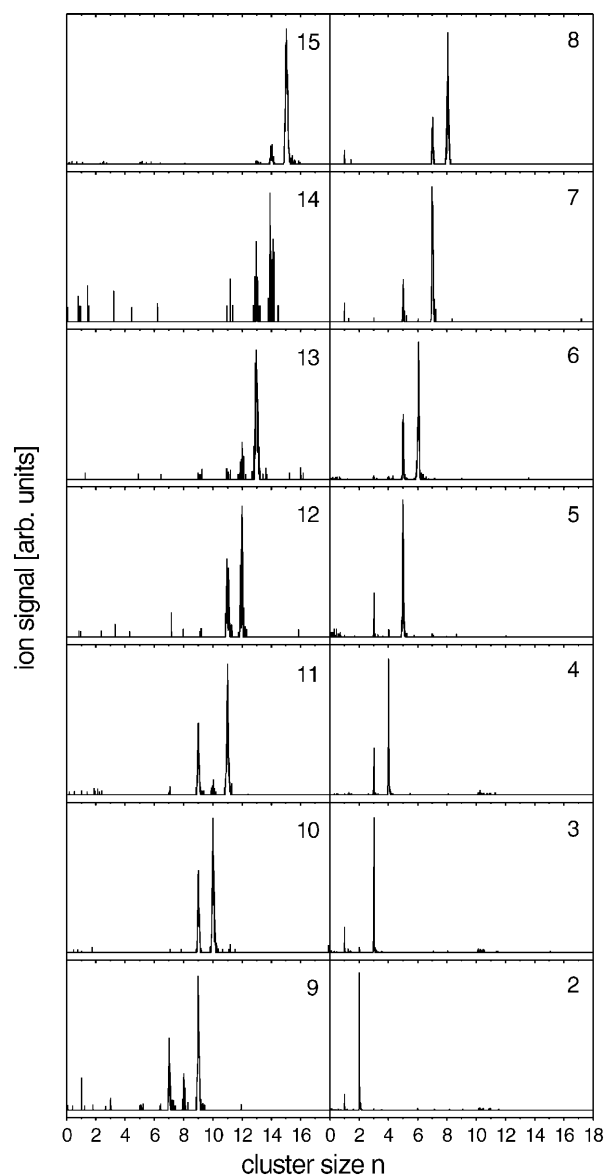


**Fig. 3.** TOF spectra of  $\text{Au}_n^-$  ( $n = 2 - 15$ ) after collisional activation adjusted to energies with respect to the appearance of the first fragment.

## 4 Discussion

### 4.1 Fragmentation of gold cluster anions

Monomer and dimer evaporation are the preferred decay pathways of gold cluster anions after collisional activation with a noble gas. This has already been observed for positively charged gold clusters [13]. The odd-sized gold cluster ions have an even number of atomic valence electrons which, due to size-dependent deformations, lead to a higher stability than that of their even-sized neighboring clusters. The odd–even effect is strongest for small clusters, and vanishes with increasing cluster size. This is well known for simple monovalent metal clusters, which also exhibit shell effects [24, 25].

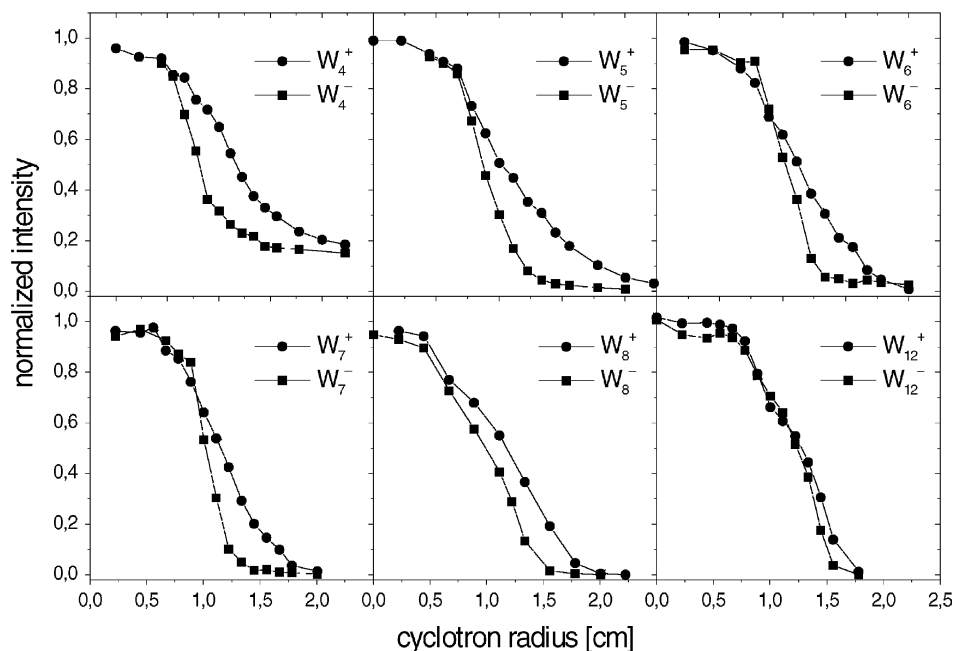


**Fig. 4.** Signal intensities of  $W_n^+$  and  $W_n^-$  ( $n = 4 - 8$  and  $12$ ) as a function of cyclotron radius after collisional activation. The data points are connected to guide the eye.

As derived in detail in [13] by energy arguments on the basis of a Born–Haber cycle, neutral dimer evaporation is the preferred decay channel of  $Au_n^+$  whenever the dissociation energy for monomer evaporation of the next-smallest cluster  $Au_{n-1}^+$  is below the dissociation energy of the neutral dimer. The same argument holds for anionic clusters. Thus, the present observations show that the dissociation energies of the even-sized anionic clusters for  $n \leq 11$  are below that of the neutral dimer, while the energies of all other clusters are higher.

The largest gold clusters decaying mainly by dimer evaporation are  $Au_{11}^-$  and  $Au_{13}^+$  [13]. Both of these species have 12 atomic valence electrons. This is another indication that the evaporation mechanism of gold clusters is largely determined by their electronic structure.

As mentioned above, the total gold cluster intensity has been found to decrease as a function of excitation. There are two possible explanations: (i) After excitation the motion of the clusters is not slowed down enough by the collisions, i.e., the clusters’ cyclotron radius remains larger than the radius of the hole in the endcap of the trap, thus they cannot be ejected from the trap for subsequent time-of-flight mass spectrometry; (ii) there is an alternative decay channel which reduces the number of anions: electron emission. In order to decide this question, a direct comparison with cationic clusters has to be performed. While it has not been studied for the case of gold, the question of electron emission of tungsten clusters is addressed explicitly in the following section.

## 4.2 Electron emission of tungsten cluster anions

The lack of fragment products for  $W_n^\pm$  agrees with earlier photoexcitation experiments on neutral and anionic tungsten clusters [4, 5]. Model calculations estimate for  $n \leq 21$

a dissociation energy above 6 eV [26], higher by far than the experimentally determined electron affinity, which is around 2 eV [27]. Obviously, the inner energy of the cations obtained by collisional activation is not high enough to induce fragmentation.

As indicated above, there is some loss of cluster signal intensity at large cyclotron excitation, since not all ions can leave the trap to be detected. While the decrease of the  $W_n^+$  signal (which is not affected by electron emission) as a function of excitation can be attributed to this phenomenon, the additional signal loss of  $W_n^-$  (Fig. 4) is explained by electron emission.

Earlier time-resolved laser experiments [5] have shown that there is a significant contribution of thermionic emission along with the possibility of “direct” electron detachment. Note that activation by collisions with neutral atoms means vibrational excitation and thus heating of the clusters. Therefore, no electrons are expected from a direct electronic excitation process. While the present experiments have not involved any time resolution, it has been observed that with increasing cluster size, the  $W_n^-$  curves resemble more and more the ones of the cations (Fig. 4). It seems that the larger clusters, which have more internal degrees of freedom and thus lower emission rates, do not have the time (even after the storage period of 1 s) to emit an electron.

## 5 Conclusion and outlook

Collisionally activated gold and tungsten clusters,  $Au_n^-$  and  $W_n^-$ , have been observed to decay by monomer/dimer evaporation and electron emission, respectively. The dissociation pathways of the anionic gold clusters resemble those of their isoelectronic cationic counterparts,  $Au_{n+2}^+$ ,

i.e., they give evidence of the importance of the electronic structure. Neither the positively charged nor the negatively charged tungsten clusters exhibit any fragmentation. The small tungsten cluster anions, however, emit electrons, which is likely to be a thermionic process. We intend to investigate further anionic clusters and to compare their behavior upon collisional and laser activation. In particular, studies of systems where the electron affinity is similar to the dissociation energy will be of interest, since these clusters may exhibit the simultaneous population of both decay channels.

The project has been supported by the Deutsche Forschungsgemeinschaft and the Materialwissenschaftliches Forschungszentrum Mainz. H.W. acknowledges the financial help of the European community within the TMR program and the EUROTRAPS network (FMRX-CT97-0144 (DG12-MIHT)). P.L. is a Postdoctoral Researcher of the Fund for Scientific Research – Flanders (F.W.O.).

## References

1. C. Bréchnignac *et al.*: J. Chem. Phys. **101**, 6992 (1994)
2. M.F. Jarrold *et al.*: J. Chem. Soc. Faraday Trans. **86**, 2537 (1990)
3. B.A. Collings *et al.*: J. Chem. Phys. **99**, 4174 (1993)
4. T. Leisner *et al.*: J. Chem. Phys. **99**, 9670 (1993)
5. H. Weidele *et al.*: Surf. Rev. Lett. **3**, 541 (1996)
6. G. Ganteför *et al.*: Phys. Rev. Lett. **77**, 4524 (1996)
7. K.H. Hansen, O. Echt: Phys. Rev. Lett. **78**, 2337 (1997)
8. R.M. Mitzner, E.E.B. Campbell: J. Chem. Phys. **103**, 2445 (1995)
9. U. Frenzel *et al.*: Z. Phys. D **40**, 108 (1997)
10. O. Echt, K. Sattler, E. Recknagel: Phys. Rev. Lett. **47**, 1121 (1981)
11. I. Rabin, C. Jackschath, W. Schulze: Z. Phys. D **19**, 153 (1991)
12. D.A. Hales *et al.*: J. Chem. Phys. **100**, 1049 (1994) and references therein
13. St. Becker *et al.*: Z. Phys. D **30**, 341 (1994); Comp. Mater. Sci. **2**, 633 (1994); Rapid Commun. Mass Spectrom. **8**, 401 (1994)
14. M.F. Jarrold, E.C. Honea: J. Phys. Chem. **95**, 9181 (1991)
15. W. Begemann *et al.*: Z. Phys. D **12**, 229 (1989)
16. M.F. Jarrold: in *Clusters of Atoms and Molecules I*, ed. by H. Haberland, 2nd edn. (Springer, Berlin 1995) p. 163
17. C.E. Klotz: Chem. Phys. Lett. **186**, 73 (1991)
18. P.M.St. John, C. Yerezian, R.L. Whetten: J. Phys. Chem. **96**, 9100 (1996)
19. C. Yerezian, K. Hansen, R.L. Whetten: Science **260**, 652 (1993)
20. L. Schweikhard *et al.*: invited ISSPIC contribution, recommended by the referees for publication in Eur. Phys. J. D
21. L. Schweikhard *et al.*: Phys. Scr. T **59**, 236 (1995)
22. L.S. Brown, G. Gabrielse: Rev. Mod. Phys. **58**, 233 (1986)
23. S. Krückeberg *et al.*: J. Chem. Phys. **110**, 7216 (1999)
24. W.A. de Heer: Rev. Mod. Phys. **65**, 611 (1993)
25. M. Manninen *et al.*: Z. Phys. D **31**, 259 (1994)
26. A.R. Miedema: Z. Metallkunde **69**, 287 (1978); Faraday Symp. Chem. Soc. **14**, 136 (1980)
27. H. Weidele *et al.*: Chem. Phys. Lett. **237**, 425 (1995)